ISSN (e): 2250 – 3005 || Volume, 07 || Issue, 06|| June – 2017 ||
International Journal of Computational Engineering Research (IJCER)

2-D Numerical Investigation of the Single Blade and Tandem Blade Rotor in Low Speed Axial Flow Compressor

M.Rajadurai*, P.Vinayagam, K.Balakrishnan, G.Mohana Priya
Assistant professor, Department of Aeronautical Engineering, Mahendra Engineering College, Namakkal-637503, India

ABSTRACT
The dual airfoil compressor rotor configuration is where two separate blades are mounted on a common rotating wheel. The premise of this study is that a dual airfoil rotor can do more work at the same loss level as a single airfoil, which would reduce the number of required stages in a compressor. While dual airfoils are commonly used in centrifugal impellers, they have yet to be applied to a commercial axial-flow rotor. This project presents some results of a 2-D computational study of the axial dual configuration in a fully subsonic flow field. This project also includes the numerical investigation of the steady, two-dimensional flow field in a tandem compressor cascade. The interaction mechanism has been investigated between the two blades. The comparison has been made based on the static and total pressure distribution along the blades.
Keywords: *compressor, tandem airfoil, cascade, high-loading, tandem blade, rotor, computational.*

I. INTRODUCTION

The axial-flow compressor designers should face the challenges is that of using as few stages as possible to achieve the desired pressure rise without compromising efficiency. The obvious benefits to using fewer stages are improved engine power-to-weight ratio and a reduction in manufacturing parts. For example, a typical stage in a 9-stage subsonic compressor will have a pressure ratio (PR) of around 1.22. By using dual airfoils in the last two stages, it may be possible to increase their individual Pressure ratios to a level such that only eight stages---six conventional and two dual---are required instead of nine. It is with this ultimate goal in mind that the present research has been undertaken.

While there is a fair amount of literature on the subject, much of it focuses on a particular geometry or very specific flow conditions. From the designer's standpoint, it is desirable to have information available that summarizes more general airfoil geometries and flow conditions that are found in a compressor. This paper presents some of the results of an ongoing project that will ultimately deliver both fundamental and practical knowledge of the dual airfoil rotor. Prior to any discussion of the dual-airfoil, it is necessary to have basic understanding of the lexicon used to describe it. Fig shows a 2-D view of a dual-airfoil configuration.

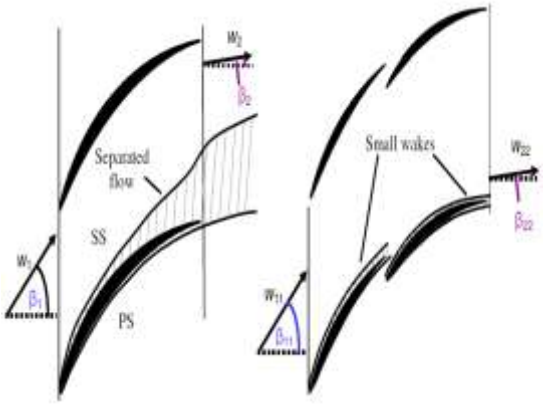

Fig. 1 2-D Profile view of highly loaded axial-flow single and tandem airfoil (R)

II. FLOW SIMULATION IN A NACA65 COMPRESSOR CASCADE

To validate the turbulence and the numerical model, a simulation of the two-dimensional flow field in a linear compressor cascade at various incidences was developed. Seven different inlet flow angles, varying from high positive incidence to high negative incidence have been simulated.

A. Cascade Geometry

The blade profile corresponds to one of the many blades experimentally tested at low speeds by Emery et al. and numerically investigated by [22] using a model with wall functions in a finite-element based pressure based solver. The geometrical parameters are summarized in Table I.

TABLE: I GEOMETRICAL PARAMETERS NACA651510

Blade geometry	Solidity	Stagger angle
NACA 651510	s/c = 1	30.48°

B. Inlet Flow Field and Operating Conditions

[7] Reported a magnitude of the inlet velocity, measured in the free stream, of about 28.956 m/s. However the analysis is non-dimensional, this velocity is used to calculate the upstream Mach number.

$$M_1 = \frac{w_1}{\sqrt{\kappa RT}} \approx 0.0845$$

Where the isentropic exponent k is 1.4, the gas constant R is 286 J/kgK and the temperature is 293 K. Since the compressibility effects of the flow has to be taken into account when the Mach number is higher than 0.2, the flow field under investigation is essentially incompressible.

The design angle of attack is fixed at 15° as indicate Fig 3 for the geometrical parameters of the blade. Thus, the inlet flow angle at design point is β=45°.

The operating conditions of the cascade are estimated using the corresponding blade Mellor diagram. Fig shows that the maximum negative and positive incidences acceptable for the stated design conditions are 39.5° and 52° respectively.

Due to the fact that Mellor specifies the blade stall when the total losses are 1.5 times the minimum losses and [12] states twice the minimum losses as the stall point; for the present simulation values slightly higher than those obtained by Mellor will be used as maximum incidences. Thus, the maximum negative incidence is set to 36° and the maximum positive incidence to 54°.

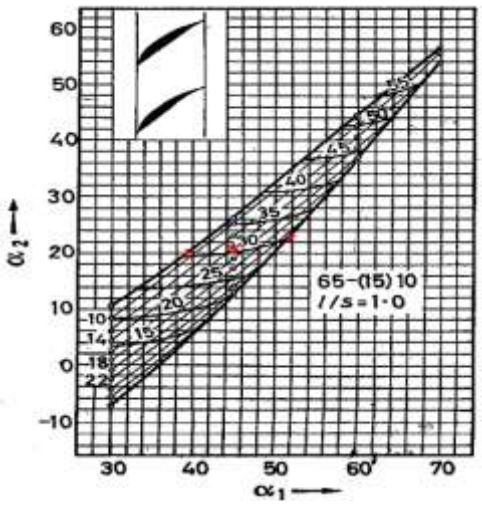

Fig: 2 Mellor diagram. NACA651510

C. Numerical Method

The set of governing equations, for a steady two-dimensional incompressible flow, was solved numerically by the non-dimensional finite element method.

1) Face Mesh: A mesh formed by a structured region near the blade surface and an unstructured region on the remainder of the computational domain was used. Fig shows the final mesh that consists approximately of 12247 elements.

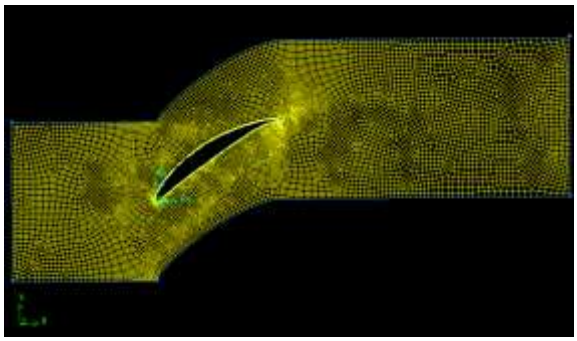

Fig: 3 Finite element mesh. NACA651510

The mesh density is higher where the velocity gradients are higher, that means in the proximities of the leading and trailing edges. Fig3 illustrates a mesh detail for the blade tested. With the boundary layer modelling the grid should be highly densified in the proximities of the walls. The wall functions model are used to capture the blade boundary layers and special consideration needs to be given to the cell size adjacent to the wall. Due to the high gradients of pressure in the vicinity of the leading and trailing edge these areas are the most critical in terms of meshing. The grid cells needs to be designed so that the skewness would be as small as possible.

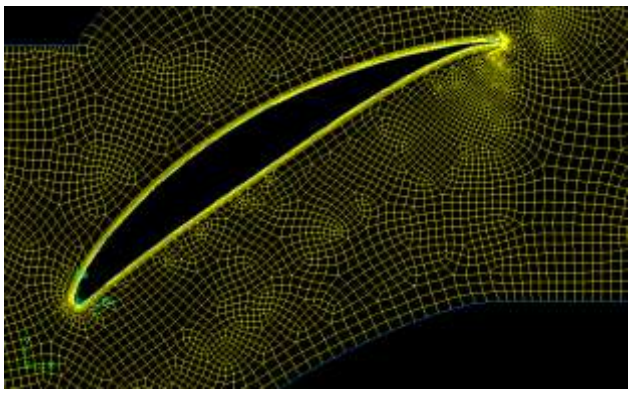

Fig: 4 Mesh detail. NACA651510

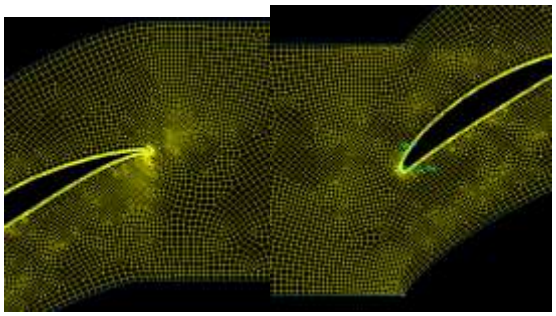

a) Leading edge b) Trailing edge

Fig: 5 Enlargement of the final mesh

A detail of the final mesh around the leading and trailing edge is illustrated in Fig 5

D. Results and Discussion

The investigation was made on the basis of the following local quantities: blade surface pressure distribution and total pressure coefficient.

1) Static Pressure Coefficient: The flow behaviour along the blade shows an initial acceleration on the suction surface up to 20% of the chord from the leading edge. Thereafter a constant deceleration of the flow towards the trailing edge is noticeable. On the pressure surface the static pressure distribution remains almost constant along the blade. The distribution of the pressure along the blade at off design incidence is plotted in Fig 6 for inlet angles of 35° and 55°. At maximum negative incidence (Fig) the stagnation point moves toward the suction side. Due to the flow around the blade leading edge, high velocities occur on the pressure side near the leading

edge, causing a separation tendency in this area. This separation tendency occurs approximately 5% of the chord and it is evident as a step in the deceleration processes that takes place in the pressure surface near the leading edge.

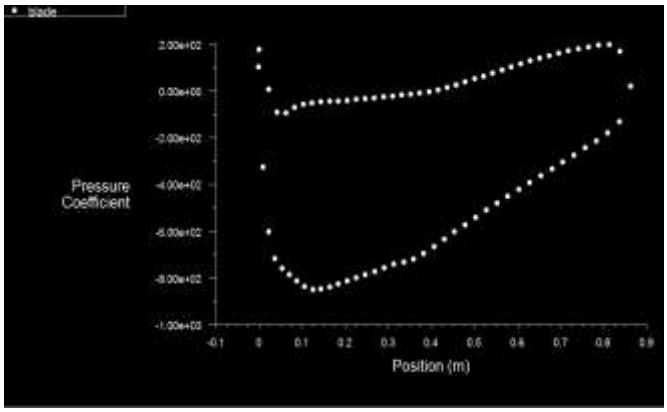

Fig: 6 Pressure coefficient and position for single blade contribution

For positive incidences the maximum pressure difference is shifted toward the front of the blade. In Fig b there is a flow separation tendency in the rear part of the blade. This tendency is due to the high diffusion process along the suction side.

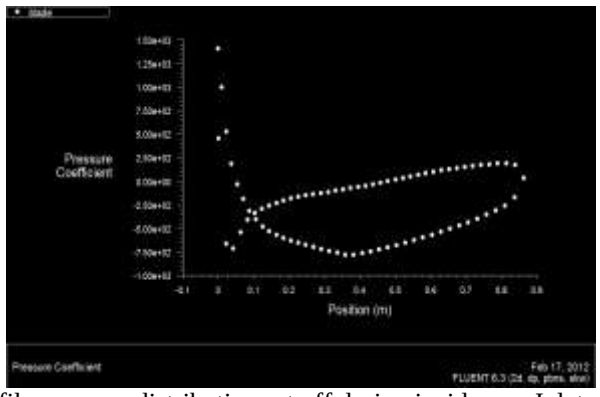

Fig: 7 Profile pressure distributions at off design incidences Inlet angle = 35°

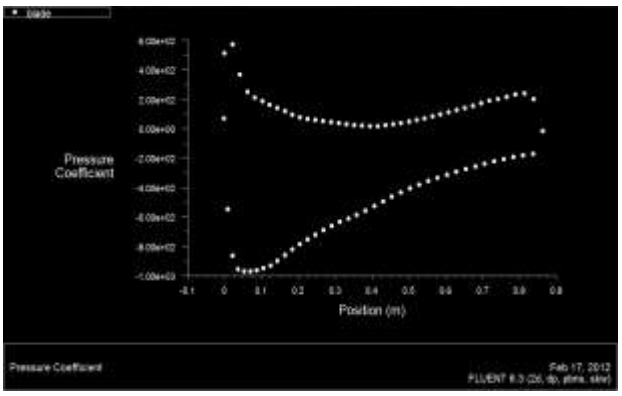

Fig: 7 Profile pressure distributions at off design incidences Inlet angle = 55°

2) Validation Summary: From the validation of the turbulence and numerical model a short summary is given before moving onto the main results. For the turbulence model it is sufficient to use the classical Ķ-ε model with wall functions as seen in the results obtained.

III. SIMULATION OF FLOW THROUGH TANDEM CASCADE

In order to recognize the interaction mechanisms between the two profiles that conform a tandem blade, a numerical simulation of a linear high turning compressor stator cascade using tandem blade rows is performed. The comparison between the blades acting independently and a tandem blade will lead to identify the mechanisms that affect the flow along the tandem arrangement. To answer the question if the numerical

computation is able to predict the main features of the tandem cascade flow field, the validation of the result is taken into account by a qualitative comparison with experimental data reported by [2]. A detailed description of the results of [2] investigation was summarized

A Inlet Conditions

The overall data at design conditions chosen for the present simulation read as follows: The incoming flow with an inlet Mach number lower than 0.2 is considered incompressible. An inlet flow angle of α=65° has to be turned 46°, thereby the flow is diffused to leave the device with an outlet angle of approximately 19° at a reasonable low total pressure loss level. The Reynolds number calculated with the inlet velocity (v1) and the chord of the first profile (Cf) is set for all the simulations to Re = 245000. Therefore, the overall Reynolds number defined with the inlet velocity (v1) and the overall chord of the tandem blade (Ct) is always higher than 450000.

Due to the many variables that influence the design of a tandem cascade, the present work will take the following assumptions to perform the investigation:

- The front and rear profiles in the tandem cascade have the same chord (Cf=Cr).
- The number of blades in the front and rear row of the cascades is the same. That means that the solidity of the front blade row, defined as (σ1=Cf/s) , is equal to the solidity of the second blade row (σ2=Cr/s).

The guideline used to choose the profile geometry was influenced by the results reported by [25] .Thus, a tandem blade with approximately 50-50 % loading split, formed by a low cambered first blade NACA651210 that deflect the flow roughly 15° and a high cambered second blade NACA652110 responsible for the remained flow deflection of more than 30°, was chosen. The stagger angle for both blades was calculated at design point using blade's Mellor diagram. Detailed cascade blade geometry is summarized in Table II.

TABLE: II TANDEM CASCADE BLADE GEOMETRY.

Blade variables	**Front lade**	**Rear blade**
Blade profile	NACA 651210	NACA 65210
Stagger angle	55°	30°
Solidity [-]	σ1=1	σ2=1

B. Initial Configuration

The first step in the investigation is to characterize the flow when there is no influence between the two blades that conform the tandem cascade. This is achieved by setting the axial displacement of the rear profile to a high value denoted as "a = infinite". In this case the whole arrangement will be treated as two isolated blades. Thus, two different models (related to each profile) are evaluated and the results are compiled into an equivalent tandem blade with high axial displacement.

1) Finite Element Mesh: The mesh generated for each tandem configuration was developed using a GAMBIT mesh algorithm. Due to the fact that each model needs a different mesh, it results inconvenient to show the mesh for all the tandem blades tested. Therefore, only one representative mesh corresponding a tandem blade with an axial displacement of 0 and a tangential displacement of 0.2 is shown in Fig 8.

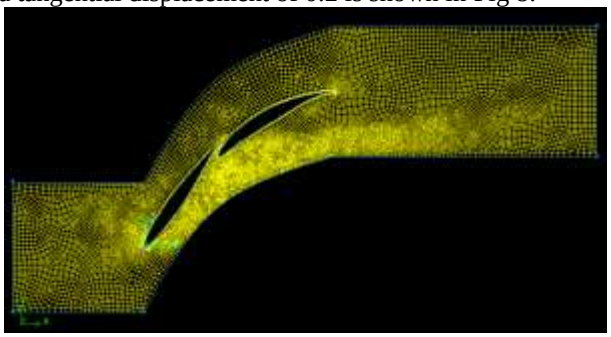

Fig.8 Tandem mesh tandem blade with a=0 and t=0.2

Fig a and Fig b show grid details of a tandem blade with a=0 and t=0.2

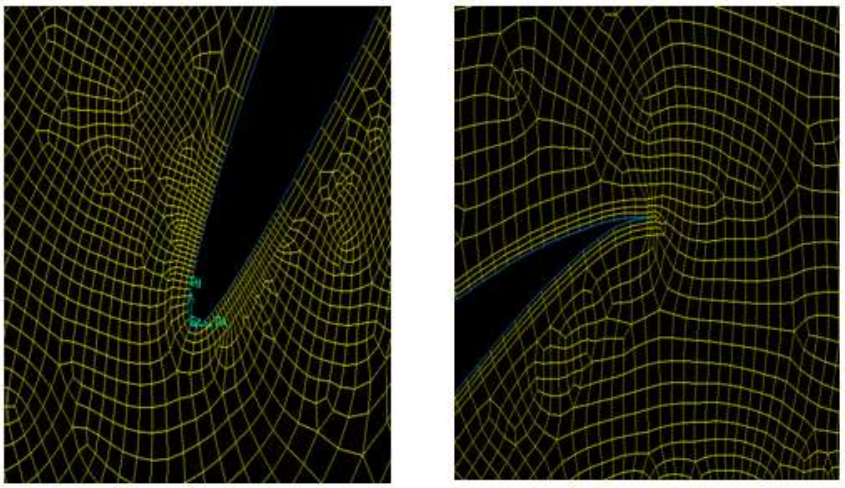

Fig: 9 First profile LE and second profile TE detail for a tandem blade with a=0 and t=0.

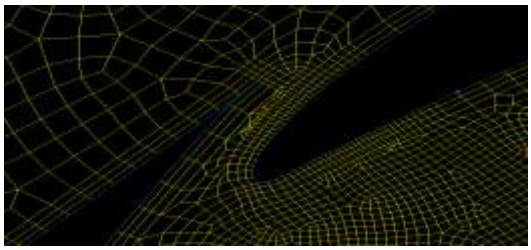

Fig: 10 Grid detail for a tandem blade with a=0 and t=0.2

In this section the influence of the relative blade position when there is no gap nozzle effect is discussed. The comparison between the results obtained and the corresponding tandem blade with a= infinite will lead to identify the main character is tics of the tandem configurations. Static pressure distribution, Dynamic pressure distribution and Total pressure distribution are the bases of the study.

C. Pressure Coefficient

Fig11. Show the static pressure coefficient the blade with a=0 and t=.02 is characterized numerically. The Fig shows that the flow behaviour along the suction surface of the first profile is not affected by the relative position of the rear blade. This characteristic is explained as a consequence of the no interaction between the blades in this surface.

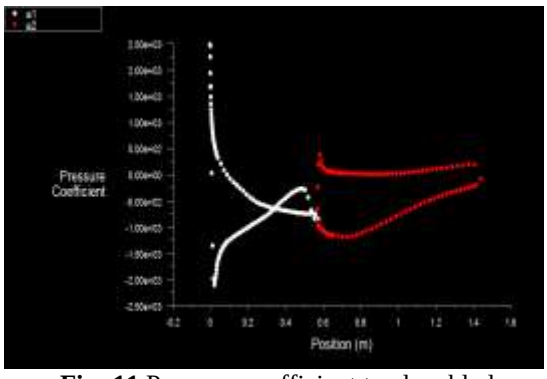

Fig: 11 Pressure coefficient tandem blades

The simulations of the tandem blades with the rear profile located in the viscous free zone showed that the flow along the pressure surface of the front profile is slightly more decelerated than the corresponding tandem blade with high axial displacement (a= inf). This is due to the presence of the second profile in the proximities of the trailing edge of the front blade.

The pressure distribution along the second profile shows that the maximum pressure difference is shifted toward the leading edge of the blade. That means that the flow incidence of the rear profile is higher than the tandem blade with a= inf (this phenomenon is expected to increase for lower values of axial displacements and to

decrease for higher values). Although the incidence is higher, the maximum pressure difference does not vary respect to the blade with high axial displacement. This is a consequence of the interaction between of the wake of the first profile and the velocity field in the vicinity of the suction surface of the rear blade. This phenomenon is illustrated with the velocity contours of a tandem blade with a=0and t=0.2 in Fig 12. The velocity contours and velocity vectors for a tandem blade a=0and t=0.2 are presented in Fig12 and Fig 13. In both Figs it can be seen the separation at the rear blade suction surface.

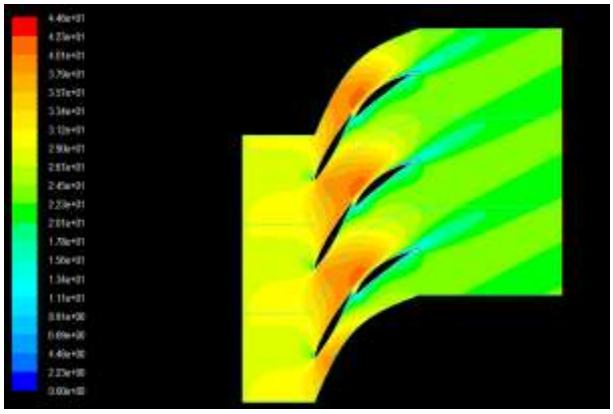

Fig: 12 Velocity contours. Tandem blade with a=0 and t=0.2

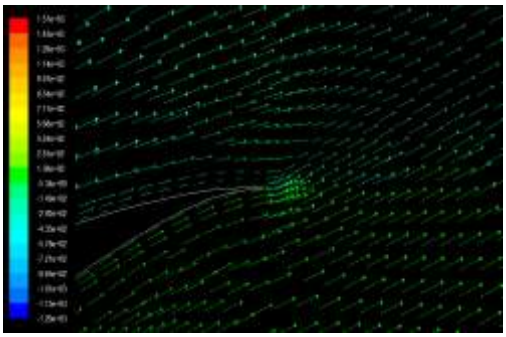

Fig: 13 Velocity Vectors. Rear profile tandem blade with a=0.2 and t=0.2

D. Results and Discussion

This part of the investigation has been conducted to assess the advantage of a tandem cascade with the presence of gap nozzle geometry between the blades as opposed to the two single blades acting independently. The study is made on the bases of the static pressure distribution along the blades, the dynamic pressure distribution and the total pressure at one chord downstream.

1) Pressure Coefficient: The Fig there is the comparison between the two blades that conform the tandem arrangement and the corresponding single blade acting independently. There is also a specification of the gap nozzle channel limit for each blade.

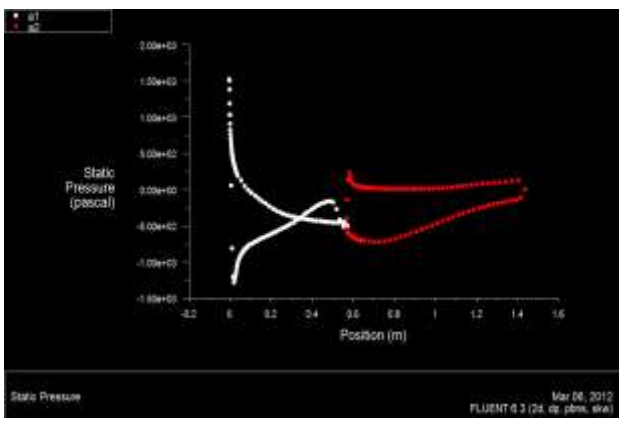

Fig: 14 Pressure coefficients. Tandem blades a=0.

2) Flow behaviour over front blade: In the tandem blades tested it was noticed that the relative position of the second profile does almost not disturb the flow along the suction surface of the front blade. This characteristic was expected because the interaction between both blades is inexistent in this surface. Thus, the flow behaviour is quite similar to the flow along the blade acting independently (an initial acceleration up to 30% of the chord from the front blade leading edge, then the flow starts diffusing constantly toward the trailing edge). Nevertheless, it was appreciable that if the tangential displacement of the second blade is quite large (that means low values of F1/F2 ratio) the flow is slightly more accelerated than the corresponding flow on the suction surface of a tandem blade with a=inf. This fact is attributed to a mass flow balance between the gap nozzle area (where the flow has low momentum) and the flow channel between two consecutive tandem blades.

On the pressure surface of the front blade it is evident that the flow is highly influenced by the gap nozzle area. This influence is presented as a blockage effect that causes a lower flow velocity in the proximities of the front blade trailing edge pressure surface. Fig illustrates a comparison between various F1/F2 ratios for the front profile of a tandem blade with a=0

The lowest velocity in the pressure surface occurs when the ratio F1/F2 is the highest. It is also appreciable that when the ratio F1/F2 increases there is also an increment in the blockage effect. The flow behaviour in this surface shows a constant deceleration up to the gap channel limit. Thereafter, the flow enters into the gap nozzle area and the velocity increases toward the trailing edge of the profile. This characteristic is due to the nozzle effect in the gap zone.

The comparison between the computational results of the front blade and the experimental data reported by [2] in Fig shows that the numerical method predicts quite well the flow characteristics along the blade. Thus, Fig shows the same flow behaviour as the measurements.

3) Flow behaviour over rear blade: The pressure surface static pressure distribution of the second blade shows that for large tangential displacements (low values of F1/F2) the inlet incidence angle of the profile is higher compared with the corresponding tandem blade with a=inf.

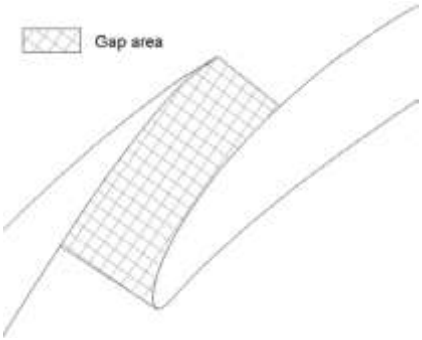

Fig: 15 Convergent-divergent gap

This phenomenon is attributed to the fact that the flow is not still totally deflected by the front profile. Therefore, it is expected an increment in the incidence of the rear blade proportional to the relative axial distance. Fig shows the path flow for a tandem blade with a=0and F1/F2=0.2.

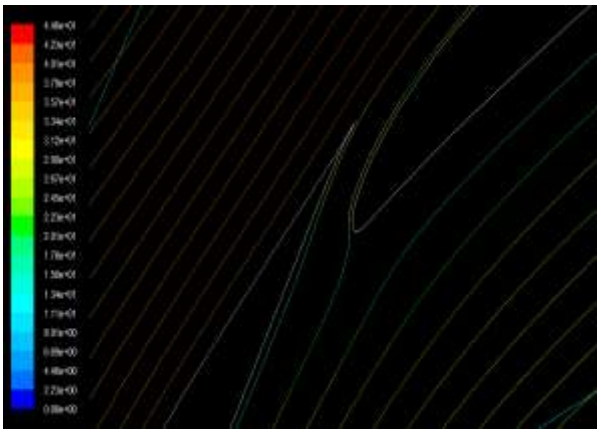

Fig: 16 Path flow lines. Tandem blade with a=-0 and F1/F2=0.

In the Fig it is evident that the inlet angle is higher than the design inlet angle calculated with the velocity field of the front profile one chord downstream in a tandem blade with a=∞.

IV. FUTURE ENHANCEMENT

Future work will focus on further refining the tandem configuration with the ultimate goal of having a dual airfoil that will outperform the single airfoil at all loading conditions. The final step will be to perform wind tunnel tests on select configurations for the purpose of data validation.

V. CONCLUSIONS

In the present investigation an attempt has been made to understand the flow behavior along the two profiles that conform a tandem arrangement. The chosen tandem concept with a tandem blade conformed by two NACA65 profiles with 1:1 blade number ratio and the same chord length between both blades fulfill the design goal of 46° flow turning under 2D flow conditions. At the beginning, it could be though to use a single blade to meet the require targets but the high flow deflection results inconvenient due to the imminent flow separation on the suction surface of the blade. Thus, it is concluded that the deflection capabilities of tandem blades are higher compared with single profiles.

REFERENCES

[1] Abbot, I.H., Von Doenhoff, A.E., Theory of Wing Sections, 1959, Dover Publications, New York.
[2] Bammert, K., Staude, R., Experimentelle Untersuchungen an ebenen verzögernden Tandemgittern, 1976, VDI-Berichte Nr. 264, Pg. 81 – 89, Hannover.
[3] Bruun, H. H., Hot-wire Anemometry, 1995, Oxford University Press. United States of America.
[4] Cumpsty, N. A., Compressor Aerodynamics, 1989, Longman Group, New York.
[5] FLUENT, FLUENT 6 User´s Manual, 1998, Fluent Inc.
[6] GAMBIT User´s Manual.
[7] Emery, J.C., Herrig, L. J., Erwin, J. R., Felix, A.R., Systematic Two-Dimensional Cascade Test of NACA 65-Series Compressor Blades at Low Speeds, 1958, NACA Report 1368.
[8] Horlock, J. H., Axial Flow Compressor, 1973, Kreiger Publishing Co., Melbourne, FL.
[9] Hughes, W., Gaylord, W., Basic Equations of Engineering Science, 1964, Schaum´s Outline Series, McGraw-Hill, New York.
[10] Ihlenfeld, H., Strömungsvorgänge an geraden, stark verzögernden Spaltflügelgittern, 1965, Maschinenbautechnik 14 Heft 7, Pag 361- 365.
[11] Lakshminarayana, B., Fluid Dynamics and Heat Transfer, 1996, Wiley-Interscience, United States of America.
[12] Lieblein, S., Diffussion Factor for Estimating Losses and Limiting Blade Loadings in Axial Flow Compressor Blade Elements, 1953, NACA Research Memorandum RM E53D01.
[13] Lieblein, S., Loss and Stall Analysis of Compressor Cascades, 1959, Journal of Basic Engineering, Pag. 387 – 400.
[14] Patankar, S.V., Numerical Heat Transfer and Fluid Flow, 1980, Hemisphere Publishing Corporation.
[15] Roberts, D., Kacker, C., Numerical Investigation of Tandem-Impeller Designs for a Gas Turbine Compressor, 2002, Journal of Turbomachinary, Pag. 124.
[16] Sachmann, J., Fottner, L., Highly Loaded Tandem Compressor Cascade with Variable Camber and Stagger, 1993, ASME paper number 93-GT-235.
[17] Saha, A. K., Roy, B., Experimental Analysis of Controlled Diffusion Compressor Cascades with Single and Tandem Airfoils, 1995, ASME paper number 95-CTP-41.
[18] Saha, A. K., Roy, B., Experimental Investigations on Tandem Compressor Cascade Performance at Low Speeds, 1997, Experimental Thermal and Fluid Science, Vol 14. Pag. 263-276.
[19] Sheets, E., Multiple Row Blades for Blowers, 1988, ASME paper number 88-GT-124.
[20] Skoda, R., Numerische Simulation abgelöster und transitionaler Strömungen in Turbomaschinen, 2003, Technische Universität München, Germany
[21] Tisch, G. Numerische Simulation in einen Tandemgitter, 1998, Internal Report, Vienna University of Technology, Austria.
[22] Trenker, M., Berechnung der ebenen turbulenten Strömung in einem NACA 65 Verdichtergitter, 1997, Diploma thesis, Vienna University of Technology, Austria.
[23] Turanskyi, L., Voss, H., Über die Entwicklungsarbeiten an Tandemgitterstufen für Industrie-Axialkompressoren, Thermische Strömungsmaschinen ´85, 1985, Pag. 403 – 420, Bochum Germany.
[24] Weber, A., Steinert, W., Design, Optimization, and Analysis of a High-Turning Transonic Tandem Compressor Cascade, 1997, ASME paper number 97-GT-412.
[25] Wennerstrom, A. J., Highly Loaded Axial Flow Compressors: History and Current Developments, ASME J. of Turbomachinery 112, 1990, Vol. 112. Pag 567 – 578.
[26] JONATHAN McGLUMPHY., 2-d Computational Studies Of Subsonic Axial-Flow Compressor Rotors Incorporating Dual Airfoils, Virginia Polytechnic Institute and State University, Blacksburg, VA 24061